Journal of Advances in Mathematics and Computer Science

Volume 38, Issue 1, Page 1-19, 2023; Article no.JAMCS.94692

ISSN: 2456-9968

(Past name: British Journal of Mathematics & Computer Science, Past ISSN: 2231-0851)

Mathematical Modelling on Impact of Interventions in the Spread of Covid-19 in Kenya

Lucas M. Mwangi [a*] **and Winifred N. Mutuku** [a]

[a] *Department of Mathematics and Actuarial Science, Kenyatta University, Kenya.*

Authors' contributions

This work was carried out in collaboration between both authors. Both authors read and approved the final manuscript.

Article Information

DOI: 10.9734/JAMCS/2023/v38i11737

Open Peer Review History:
This journal follows the Advanced Open Peer Review policy. Identity of the Reviewers, Editor(s) and additional Reviewers, peer review comments, different versions of the manuscript, comments of the editors, etc are available here: https://www.sdiarticle5.com/review-history/94692

Original Research Article

Received: 20/10/2022
Accepted: 26/12/2022
Published: 03/01/2023

Abstract

The history of coronavirus can be traced to the 1960s when B184 and 229E coronaviruses were discovered in the nasal washing of individuals with the common cold. There was no worry about such viruses until 2003 when the first major outbreak of SARS was discovered in southern China. The recent outbreak was in 2019 when a major outbreak of COVID-19 strain started in China. The World Health Organisation proclaimed COVID-19 as a pandemic in March 2020. Ever since this pandemic, several attempts to intervene in the spread has been tried, yet the pandemic is not dying. This persistence in the pandemic might be due to the presence of asymptomatic individuals. This unending pandemic has hit the Kenya economy badly. In this study, we mathematically investigate the effect of governmental and non-governmental intervention on the spread of COVID-19 in Kenya. To capture the effect of intervention effectively, the model considers the presence of asymptomatically infected individuals in the Kenya. The basic reproduction number is obtained using the next-generation matrix and the local stability of the equilibrium points are established.

**Corresponding author: E-mail: lucasmuiruri16@gmail.com;*

The effects of intervention on the spread of COVID-19 are simulated and illustrated as graphs. The results indicate that intervention in form awareness and public sensitisation reduces the Exposed class, Infected Classes and COVID-19-related death.

Keywords: Coronavirus; transmissions; outbreak; infected class; symptomatic dynamics; mathematical modelling.

Nomenclatures

$S(t)$:	Susceptible class
$E(t)$:	Exposed class
$I_a(t)$:	Asymptomatic Infected class
$R(t)$:	Recovered class
$I_s(t)$:	Symptomatic Infected class
$D(t)$:	Death class
$\Lambda(t)$:	influx to the population at any time
δ :	Rate of recovery from the Exposed class
α :	Rate of interaction between infected and non-infected individual
β :	Rate of infection
p :	The proportion of infected class showing symptoms
γ :	Rate of symptomatic experience
λ_1 :	the recovery rate for the asymptomatic infected class
λ_2 :	the recovery rate for the symptomatic infected class
η :	Rate of diseases-related death
μ :	rate of natural death

1 Introduction

The spread of COVID-19 has reached all countries on the planet earth except a few islands and two controversial countries. The only islands that have not recorded any case of COVID-19 are American Samoa, Cook Islands, Federated States of Micronesia, Kiribati, Nauru, Niue, Pitcairn Islands, Saint Helena, Tokelau, Tonga and Tuvalu. The two non-islands are North Korea and Turkmenistan. Most island countries have not recorded more than 20 cases (as the case of Solomon Islands). Based on the available data, most scientists agree that the separation of the islands from lands is one important factor that has prevented the massive spread of COVID-19 in the island countries. Another factor is that these islands maintained large restrictions on immigration. Apart from the two non-island countries of North Korea and Turkmenistan, all non-island countries have had their own share of the COVID-19 outbreak. Kenya as a non-island country is also going through a delicate time in its economy due to the extreme measures that have been taken to curtail the spread of the coronavirus pandemic [1, 2, 3, 4]. The Kenyan government, just like several other countries in the world, initiated the lockdown in the country in the year 2020 to control the spread of the coronavirus disease. A huge amount of money was pumped into creating awareness about the nature of the virus, the mode of transmission and the ways to prevent getting infected. Besides the sensitisation from the government angle, several individuals and groups also invested so much money to ensure that the sensitisation gets to every Kenyan. Despite the heavy awareness and sensitization to educate people and get them tested to know their COVID-19 status, a large percentage of the population has refused to get tested. Avoiding getting tested indicates that many might be infected without knowing, especially when the symptoms are not yet showing. This class of infected individuals who are not showing any symptoms

of the disease yet are very dangerous to society. It is important to carry out research that assesses the probable danger inherent in having untested individuals in Kenya. The population of Kenya is estimated to be a little above 50 million, while Nigeria (the most populous country in Africa) has over 200 million population. Also, the African continent has recorded the least number of cases of COVID-19 among all the continents, and it is therefore expected that a country like Kenya should have fewer cases than Nigeria but that is not the case. Kenya has recorded over 16% more cases than Nigeria has recorded.

Coronavirus has its root in the independent experiments of [5] and [6]. [5] collected specimens of nasal washings of 23 workers of a laboratory or their family (consisting of twenty-one adults and two children) infected with the common cold and cultivated nine different rhinoviruses that could not be found using the standard techniques. These viruses were called B814 viruses. [6] independently carried out similar experiments on some students of medicine at the University of Chicago. The virus responsible for the common cold was extracted from the students' respiratory tract and a new ether-sensitive RNA virus called 229E was cultivated. The 229E was found to be antigenically unrelated to all known human myxoviruses. In an experiment by [7], it was found out that the morphology of the B814, 229E, bronchitis, mouse hepatitis, and swine gastroenteritis viruses are the same under electron microscopy. This new virus genus was named coronavirus. Extensive research has been carried out on the study of the 229E strain of the coronavirus has been studied extensively and an outbreak of 229E was found to repeat every 2-3 years and re-infection was found to be common [1]. As emphases were placed more on the 229E strain and OC43 strain, other strains of coronavirus were found to spread in humans, as well as animals, causing different respiratory problems. Pigs, cats, rats, rabbits, mice are some of the animals in which different strains of coronavirus were discovered [8]. The coronavirus is later grouped into three categories; 229E virus category, OC43 virus category and avian infectious bronchitis virus category [2].

The coronavirus is a "nucleic acid of about 30kb long, positive in sense, single-stranded and polyadenylated" and an RNA virus that appears as negatively stained preparations in electron micrographs. As of today, coronavirus is the largest RNA virus known. If two coronaviruses infect the same cell at the same time, they are able to form another virus by recombining their genes. All coronaviruses grow and develop in the cytoplasm of the host cells and the host cell is destroyed afterwards. Fig. 1, shows a sample coronavirus in a medium.

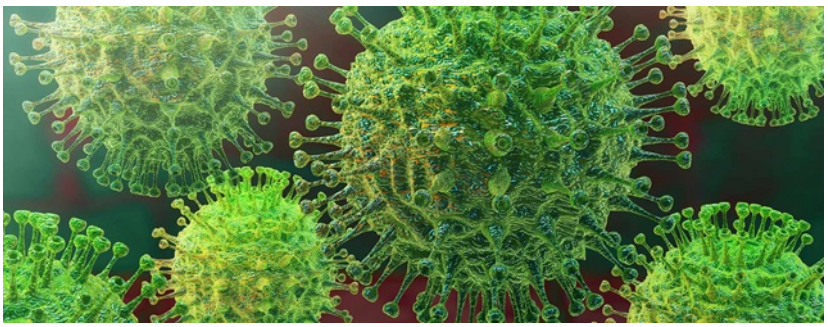

Fig. 1. The-coronavirus

The first major outbreak of coronavirus was in 2002, in Southern China. There was an outbreak of a new strain of coronavirus called severe acute respiratory syndrome (SARS) coronavirus. SARS rapidly spread to 29 countries infecting over 8000 individuals with about 800 deaths. Although the source of this virus was not certain, there were speculations that it emerged from human interactions with wild animals. The most recent outbreak of the coronavirus is the coronavirus disease 2019 (shortened to COVID-19 for brevity). The outbreak started as an epidemic in Wuhan, China. Considering the rapid rate at which COVID-19 was transmitted, WHO declared COVID-19 a pandemic on 11th of March, 2020 by the World Health Organisation [9]. It is referred to as Severe Acute Respiratory Syndrome coronavirus-2 (SARS-CoV-2) by the International Committee for Taxonomy of Viruses and there is a high tendency it originates from the bat since 96% genome sequence

identity was demonstrated between SARS-CoV-2 and Bat-CoV-RatG13 [10]. Animal-human and human-human transmissions are both possible means of COVID-19 transmissions, where human-human transmission dominates the transmission charts. The mode of transmission includes; respiratory droplets, direct and indirect physical contact with an infected individual. Research has shown that COVID-19 is airborne and that airborne transmission of COVID-19 contributed majorly to its transmission. Fig. 2, below illustrates how COVID-19 is transmitted.

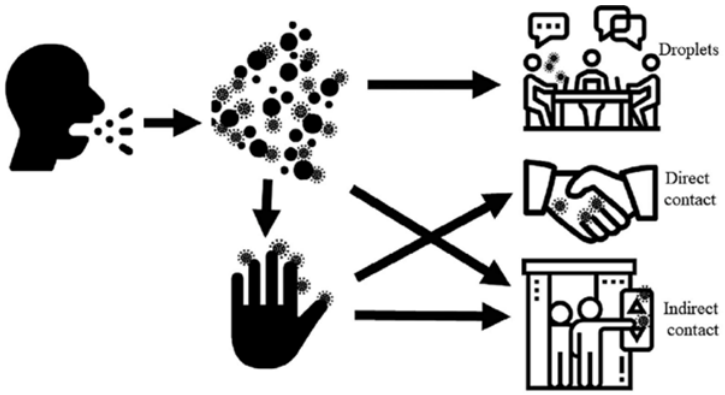

Fig. 2. Illustration-of-COVID-19

Within the last two years, a lot of researches have been carried out theoretically to combat the spread of COVID-19. In their work, [11] carried a mathematical analysis on the study of the COVID-19 outbreak in Bangladesh. The study considered the SEQIRD model which is a modification of Susceptible-Infected-Recovered (SIR) model that includes three more compartments (Quarantine Q, Exposed E, and Death D classes). The study predicts that infection in Bangladesh will increase for a period of time until the peak is reached and the rate of infection will start to decrease rapidly. A study of the COVID-19 spread in Spain, Portugal and Wuhan (in China) was carried out byNdairou2021 using fractional-time derivates. The model extends the SEQIRD model to SEQIPARD (introducing the Asymptomatic A and Rapid-Spreader classes). The study showed a good agreement with the classical integer-order time-derivative models. Meanwhile, [9] used a mathematical model to study the effect of both detection rate and possible reinfection on the spread of COVID-19 in Africa. The study shows that the fight against COVID-19 has just begun in Africa if there is a high possibility of reinfection. [12] identified the impact of immigrants on COVID-19 dynamics. The study was conducted for the entire African continent and does not specify how it affects Kenya as a country. Since it is only a speculation as to whether there is reinfection or not, this study is modification of the work of [9] with the following assumptions;

1. There are only speculations as to whether reinfection is possible or not. Cases that have been recorded are too few to consider reinfection as a major problem, hence we set the reinfection rate to zero in this present study.
2. The study considered Africa as a single continent, but in this study, the focus shall be placed on Kenya as an individual country.
3. The previous study did not consider individuals whose immunities are strong enough to combat the disease. In this study, we have included the possibility of individuals to move from the Exposed Class to the Recovered Class.
4. The spread parameters shall be chosen based on the impact of intervention to combat the spread of COVID-19.

In this study, a mathematical analysis of the spread of COVID-19 is carried out to investigate the spread of COVID-19 in a population where asymptomatically infected individuals are present and putting into consideration the intervention of the Kenyan government.

2 Methodology

2.1 Model formulation

The population is classed into six compartments, namely; Susceptible class $S(t)$, Exposed class $E(t)$, Asymptomatic Infected class $I_a(t)$, Symptomatic Infected class $I_s(t)$, Recovered class $R(t)$, and the disease-induced Death class $D(t)$. The model assumes that the influx to the population at any time t is $\Lambda(t)$, from which the Susceptible class at any time t is $S(t)$. We assume that the interaction between infected individuals and the Susceptible class happens at a rate of α, hence the proportion of the Susceptible population migrate to the Exposed class at the rate α. The Exposed class get infected at the rate β where a proportion p shows symptoms while the remaining $(1-p)$ proportion shows no symptoms. The Exposed class individuals who possess good immunity can also recover naturally at the rate δ. The Asymptomatic class becomes symptomatic at the rate of γ. The asymptomatic infected class recover at the rate λ_1 while the symptomatic class recover at a rate λ_2. It is assumed that the disease-related death is at the rate η and the natural death rate is μ. Fig.3, shows the flow chart of the transition of COVID-19 from one class to the next. The Death class is the only absorbing class, where an individual that enters cannot exit. The values of the spread parameters $\alpha, \beta, \mu, p, \lambda_1, \lambda_2$ and γ are chosen based on the current intervention from the Kenyan government.

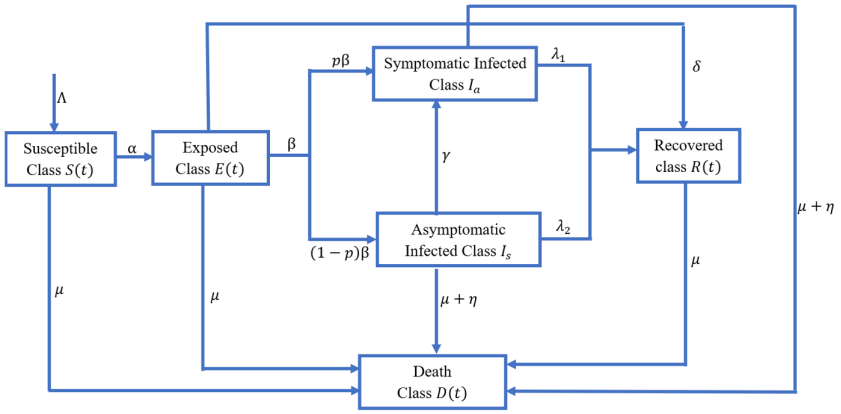

Fig. 3. Flowchart-for-COVID-19

The model governing the dynamics of COVID-19 with the six given classes is given as

$$\frac{dS}{dt} = \Lambda - \alpha\left(I_a + I_s\right)S - \mu S, \tag{2.1}$$

$$\frac{dE}{dt} = \alpha\left(I_a + I_s\right)S - \left(\beta + \mu + \delta\right)E, \tag{2.2}$$

$$\frac{dI_a}{dt} = p\beta E + \gamma I_s - \left(\lambda_1 + \mu + \eta\right)I_a, \tag{2.3}$$

$$\frac{dI_s}{dt} = \left(1-p\right)\beta E - \left(\gamma + \lambda_2 + \eta + \mu\right)I_s, \tag{2.4}$$

$$\frac{dR}{dt} = \delta E + \lambda_1 I_a + \lambda_2 I_s - \mu R, \tag{2.5}$$

$$\frac{dD}{dt} = \eta\left(I_s + I_a\right). \tag{2.6}$$

Let $N(t)$ be the total population at any time t so that

$$N(t) = S(t) + E(t) + I_s(t) + I_a(t) + R(t) \tag{2.7}$$

2.2 Feasibility region and non-negativity of solution

This section establishes the region in which the solution to the model can be found and the non-negativity of the solution within the feasibility region. By adopting the analysis of [13, 14], we sum the equations (2.1) - (2.6) and get

$$\frac{d}{dt}\left(S+E+I_s+I_a+R\right)=\Lambda-\mu\left(S+E+I_s+I_a+R\right)=\Lambda-\mu N. \tag{2.8}$$

On substituting equation (2.7), it becomes

$$\frac{dN}{dt}=\Lambda-\mu N, \tag{2.9}$$

and whose solution is

$$N\left(t\right)=\frac{\Lambda}{\mu}+\left(N\left(t_0\right)-\frac{\Lambda}{\mu}\right)e^{\mu(t_0-t)}. \tag{2.10}$$

As $t\to\infty$, the solution becomes $N\left(t\right)\to\frac{\Lambda}{\mu}$. Hence, the feasible region $\mathcal{R}$ for the system is

$$\mathcal{R}=\left\{\left(S,E,I_a,I_s,R,D\right)\in\mathbb{R}_+^5\mid N\left(t\right)\leq\frac{\Lambda}{\mu}\right\}. \tag{2.11}$$

Having established the feasibility region for the system, the non-negativity of the solution is sought. Any solution of the system (2.1 - 2.6) remains in the positive region for all initial conditions $S\left(0\right)>0$, $E\left(0\right)>0$, $I_a\left(0\right)>0$, $I_s\left(0\right)>0$, $R\left(0\right)>0$, and $D\left(0\right)>0$.

Proof. From equation (2.1),

$$\frac{dS}{dt}=\Lambda-\alpha\left(I_a+I_s\right)S-\mu S\geq-\mu S.$$

Solving the equation using separation of variable gives

$$S\geq S\left(0\right)\exp\left(\mu\left(t-t_0\right)\right)>0,\ \text{if } S\left(0\right)>0. \tag{2.12}$$

From equation (2.2),

$$\frac{dE}{dt}=\alpha\left(I_a+I_s\right)S-\left(\beta+\mu+\delta\right)E\geq-\left(\beta+\mu+\delta\right)E$$

Solving the equation using separation of variable gives

$$E\geq E\left(0\right)\exp\left(\left(\beta+\mu+\delta\right)\left(t-t_0\right)\right)>0,\ \text{if } E\left(0\right)>0. \tag{2.13}$$

From equation (2.3),

$$\frac{dI_a}{dt}=p\beta E+\gamma I_s-\left(\lambda_1+\mu+\eta\right)I_a>-\left(\lambda_1+\mu+\eta\right)I_a$$

Solving the equation using separation of variable gives

$$I_a\geq I_a\left(0\right)\exp\left(\left(\lambda_1+\mu+\eta\right)\left(t-t_0\right)\right)>0,\ \text{if } I_a\left(0\right)>0. \tag{2.14}$$

From equation (2.4),

$$\frac{dI_s}{dt}=\left(1-p\right)\beta E-\left(\gamma+\lambda_2+\eta+\mu\right)I_s>-\left(\gamma+\lambda_2+\eta+\mu\right)I_s$$

Solving the equation using separation of variable gives

$$I_s\geq I_s\left(0\right)\exp\left(\left(\gamma+\lambda_2+\eta+\mu\right)\left(t-t_0\right)\right)>0,\ \text{if } I_s\left(0\right)>0. \tag{2.15}$$

From equation (2.5),

$$\frac{dR}{dt}=\delta E+\lambda_1 I_a+\lambda_2 I_s-\mu R>-\mu R$$

Solving the equation using separation of variable gives

$$R\geq R\left(0\right)\exp\left(\mu\left(t-t_0\right)\right)>0,\ \text{if } R\left(0\right)>0. \tag{2.16}$$

From equation (2.6),

$$\frac{dD}{dt} = \eta \left(I_s + I_a \right).$$

Using the inequalities (2.14) and (2.15), then

$$\frac{dD}{dt} \geq \eta \left(I_s \left(0 \right) \exp \left(\left(\gamma + \lambda_2 + \eta + \mu \right) \left(t - t_0 \right) \right) + I_a \left(0 \right) \exp \left(\left(\lambda_1 + \mu + \eta \right) \left(t - t_0 \right) \right) \right).$$

On integrating both sides,

$$\begin{aligned} D \quad \geq \quad & D \left(0 \right) + \frac{\eta I_s \left(0 \right)}{\gamma + \lambda_2 + \eta + \mu} \left(\exp \left(\left(\gamma + \lambda_2 + \eta + \mu \right) \left(t - t_0 \right) \right) - 1 \right) \\ & + \frac{\eta I_s \left(0 \right)}{\gamma + \lambda_2 + \eta + \mu} \left(\exp \left(\left(\gamma + \lambda_2 + \eta + \mu \right) \left(t - t_0 \right) \right) - 1 \right) > 0 \end{aligned}$$

Hence, the solution space is

$$\left\{ \left(S, E, I_a, I_s, R, D \right) \in \mathbb{R}_+^6 \ \ni \ S + E + I_a + I_s + R + D \leq \frac{\Lambda}{\mu} \right\}$$

■

2.3 Equilibrium points

The works of [15, 16] and [17] show a procedure for finding the equilibrium points. By setting each of equations (2.1 - 2.7) to zero ([18]),

- the disease-free equilibrium point (DFE or e_0) is obtained by setting $I_a = I_s = E = 0$ e_0 as

$$e_0 = \left(S, E, I_a, I_s, R, D \right) = \left(\frac{\Lambda}{\mu}, \ , 0 \ , 0 \ , 0 \ , 0 \ , 0 \right).$$

- The endemic equilibrium point $e_1 = \left(S^*, E^*, I_a^*, I_s^*, R^*, D^* \right)$ is obtained as

$$\begin{aligned} S^* &= \frac{\Lambda}{\alpha \left(I_a^* + I_s^* \right) + \mu}, \ E^* = \frac{\alpha \left(I_a^* + I_s^* \right) \Lambda}{\left(\beta + \mu + \delta \right) \left(\alpha \left(I_a^* + I_s^* \right) + \mu \right)} \\ I_s &= I_s^*, \ I_a = I_a^*, \ R^* = \frac{1}{\mu} \left(\delta E^* + \lambda_1 I_a^* + \lambda_2 I_s^* \right), \ D = D^*. \end{aligned}$$

2.4 Reproduction number

The reproduction number R_0 is the number of secondary infections that a single infected individual can cause when introduced to a susceptible population. Following the works of [15, 19, 20], the the next generation matrix is used to find the reproduction number. We start by writing

$$f = \begin{pmatrix} \alpha \left(I_a + I_s \right) S \\ 0 \\ 0 \end{pmatrix}, \ v = \begin{pmatrix} \left(\beta + \mu + \delta \right) E \\ -p\beta E - \gamma I_s + \left(\lambda_1 + \mu + \eta \right) I_a \\ -\left(1 - p \right) \beta E + \left(\gamma + \lambda_2 + \eta + \mu \right) I_s \end{pmatrix}$$

and $F = \nabla f, V = \nabla v$ becomes

$$F = \begin{pmatrix} 0 & \alpha S & \alpha S \\ 0 & 0 & 0 \\ 0 & 0 & 0 \end{pmatrix}, \ V = \begin{pmatrix} \left(\beta + \mu + \delta \right) & 0 & 0 \\ -p\beta & \left(\lambda_1 + \mu + \eta \right) & -\gamma \\ -\left(1 - p \right) \beta & 0 & \left(\gamma + \lambda_2 + \eta + \mu \right) \end{pmatrix}.$$

From which the spectral radius of FV^{-1} is

$$R_0 = \frac{\alpha S \beta \left(p\lambda_2 - p\lambda_1 + \eta + \gamma + \lambda_1 + \mu \right)}{\left(\beta + \mu + \delta \right) \left(\lambda_1 + \mu + \eta \right) \left(\gamma + \lambda_2 + \eta + \mu \right)}.$$

2.5 Stability of equilibrium points

Ignoring equation (2.6) since it is decoupled from the system, then the Jacobian matrix for the system (2.1 - 2.5) is

$$J = \begin{pmatrix} -\alpha\left(I_a + I_s\right) - \mu & 0 & -\alpha S & -\alpha S & 0 \\ \alpha\left(I_a + I_s\right) & -\left(\beta + \mu + \delta\right) & \alpha S & \alpha S & 0 \\ 0 & p\beta & -\left(\lambda_1 + \mu + \eta\right) & \gamma & 0 \\ 0 & \left(1-p\right)\beta & 0 & -\left(\gamma + \lambda_2 + \eta + \mu\right) & 0 \\ 0 & \delta & \lambda_1 & \lambda_2 & -\mu \end{pmatrix}. \tag{2.17}$$

The DFE is locally asymptotically stable.

Proof. Evaluating the Jacobian at the DFE gives

$$J_0 = J\left(e_0\right) = \begin{pmatrix} -\mu & 0 & 0 & 0 & 0 \\ 0 & -\left(\beta + \mu + \delta\right) & 0 & 0 & 0 \\ 0 & p\beta & -\left(\lambda_1 + \mu + \eta\right) & \gamma & 0 \\ 0 & \left(1-p\right)\beta & 0 & -\left(\gamma + \lambda_2 + \eta + \mu\right) & 0 \\ 0 & \delta & \lambda_1 & \lambda_2 & -\mu \end{pmatrix}. \tag{2.18}$$

The characteristic equation $|J_0 - mI| = 0$ gives

$$\begin{vmatrix} -\mu - m & 0 & 0 & 0 & 0 \\ 0 & -\left(\beta + \mu + \delta\right) - m & 0 & 0 & 0 \\ 0 & p\beta & -\left(\lambda_1 + \mu + \eta\right) - m & \gamma & 0 \\ 0 & \left(1-p\right)\beta & 0 & -\left(\gamma + \lambda_2 + \eta + \mu\right) - m & 0 \\ 0 & \delta & \lambda_1 & \lambda_2 & -\mu - m \end{vmatrix} = 0,$$

and the eigenvalues are obtained as

$$m_1 = m_5 = -\mu,\ m_2 = -\left(\beta + \mu + \delta\right),\ m_3 = -\left(\lambda_1 + \mu + \eta\right),\ m_4 = -\left(\gamma + \lambda_2 + \eta + \mu\right).$$

Hence, the DFE is locally asymptotically stable since all eigenvalues are negative. ■ The EEP is locally asymptotically stable if $R_0 > 1$.

Proof. Evaluating the Jacobian at the EEP gives

$$J_1 = J\left(e_1\right) = \begin{pmatrix} -\alpha\left(I_a^* + I_s^*\right) - \mu & 0 & -\alpha S^* & -\alpha S^* & 0 \\ \alpha\left(I_a^* + I_s^*\right) & -\left(\beta + \mu + \delta\right) & \alpha S^* & \alpha S^* & 0 \\ 0 & p\beta & -\left(\lambda_1 + \mu + \eta\right) & \gamma & 0 \\ 0 & \left(1-p\right)\beta & 0 & -\left(\gamma + \lambda_2 + \eta + \mu\right) & 0 \\ 0 & \delta & \lambda_1 & \lambda_2 & -\mu \end{pmatrix}. \tag{2.19}$$

The characteristic equation $|J_1 - mI| = 0$ gives

$$\begin{vmatrix} -\phi_{11} - m & 0 & -\alpha S^* & -\alpha S^* & 0 \\ \phi_{21} & -\phi_{22} - m & \alpha S^* & \alpha S^* & 0 \\ 0 & p\beta & -\phi_{33} - m & \gamma & 0 \\ 0 & \left(1-p\right)\beta & 0 & -\phi_{44} - m & 0 \\ 0 & \delta & \lambda_1 & \lambda_2 & -\mu - m \end{vmatrix} = 0,$$

where

$$\phi_{11} = \alpha\left(I_a^* + I_s^*\right) + \mu,\ \phi_{21} = \alpha\left(I_a^* + I_s^*\right) = \phi_{11} - \mu,\ \phi_{22} = \left(\beta + \mu + \delta\right),$$
$$\phi_{33} = \left(\lambda_1 + \mu + \eta\right),\ \phi_{44} = \left(\gamma + \lambda_2 + \eta + \mu\right)$$

and the eigenvalues are obtained as $m_1 = -\mu$ and the remaining 4 eigenvalues are obtained from

$$(\phi_{11}+m)\begin{vmatrix} -\phi_{22}-m & \alpha S^* & \alpha S^* \\ p\beta & -\phi_{33}-m & \gamma \\ (1-p)\beta & 0 & -\phi_{44}-m \end{vmatrix} + \phi_{21}\begin{vmatrix} 0 & -\alpha S^* & -\alpha S^* \\ p\beta & -\phi_{33}-m & \gamma \\ (1-p)\beta & 0 & -\phi_{44}-m \end{vmatrix} = 0,$$

$$\Rightarrow m^4 + \Delta_3 m^3 + \Delta_2 m^2 + \Delta_1 m + \Delta_0 = 0,$$

where

$$\begin{aligned}
\Delta_3 =& \phi_{11}+\phi_{22}+\phi_{33}+\phi_{44},\\
\Delta_2 =& \phi_{11}\phi_{44}+\phi_{11}\phi_{22}+\phi_{11}\phi_{33}+\phi_{22}\phi_{44}+\phi_{33}\phi_{44}+\phi_{22}\phi_{33}-\alpha\beta S^*,\\
\Delta_1 =& \phi_{11}\phi_{22}\phi_{44}+\phi_{11}\phi_{33}\phi_{44}+\phi_{11}\phi_{22}\phi_{33}+\phi_{22}\phi_{33}\phi_{44}\\
&-((1-p)\gamma+\phi_{11}+\phi_{21}+\phi_{44}-2p\phi_{21})\alpha\beta S^*,\\
\Delta_0 =& \phi_{11}\phi_{22}\phi_{33}\phi_{44}-(1-p)\alpha\beta\gamma S^*-\alpha\beta S^*\phi_{11}\phi_{44}\\
&+\gamma(1-p)\beta\alpha S^*\phi_{21}+p\beta\alpha S^*\phi_{21}\phi_{44}-\alpha S^*(1-p)\beta\phi_{21}\phi_{33}.
\end{aligned}$$

Using Routh-Hurwitz criteria, we require

$$\Delta_3>0,\ \Delta_0>0,\ \frac{\Delta_3\Delta_2-\Delta_1}{\Delta_3}>0,\ \left(\frac{\Delta_3\Delta_2-\Delta_1}{\Delta_3}\right)\Delta_1-\Delta_3\Delta_0>0,$$

for all the roots to be negative. By the virtue of positivity of all parameters,

$$\Delta_3 = \phi_{11}+\phi_{22}+\phi_{33}+\phi_{44}>0.$$

The fourth condition $\Delta_0 > 0$ implies that

$$\begin{aligned}
&\phi_{11}\phi_{22}\phi_{33}\phi_{44}+\gamma(1-p)\beta\alpha S^*\phi_{21}+p\beta\alpha S^*\phi_{21}\phi_{44}\\
&>(1-p)\alpha\beta\gamma S^*+\alpha\beta S^*\phi_{11}\phi_{44}+\alpha S^*(1-p)\beta\phi_{21}\phi_{33}>0.
\end{aligned}$$

which is true due to the positivity of all parameters. Using the condition that $\Delta_3, \Delta_0 > 0$, then the fourth condition becomes

$$\left(\frac{\Delta_3\Delta_2-\Delta_1}{\Delta_3}\right)\Delta_1>\Delta_3\Delta_0>0\Rightarrow\frac{\Delta_3\Delta_2-\Delta_1}{\Delta_3}>0\Rightarrow\Delta_3\Delta_2-\Delta_1>0.$$

This coincides with the third condition and the four conditions are satisfied once $\Delta_3\Delta_2 > \Delta_1$, which means;

$$\begin{aligned}
&\Delta_3(\phi_{11}\phi_{44}+\phi_{11}\phi_{22}+\phi_{11}\phi_{33}+\phi_{22}\phi_{44}+\phi_{33}\phi_{44}+\phi_{22}\phi_{33})\\
&+((1-p)\gamma+\phi_{11}+\phi_{21}+\phi_{44})\alpha\beta S^*>\phi_{11}\phi_{22}\phi_{44}+\phi_{11}\phi_{33}\phi_{44}\\
&+\phi_{11}\phi_{22}\phi_{33}+\phi_{22}\phi_{33}\phi_{44}+2p\phi_{21}\alpha\beta S^*+\alpha\beta S^*\Delta_3>0,\\
&\Rightarrow\Delta_3^2\phi_{11}+\Delta_3^2\phi_{22}+\Delta_3\phi_{33}\phi_{44}+(\gamma+2\phi_{11}+\phi_{44})\alpha\beta S^*>\\
&\Delta_3(\phi_{11}^2+\phi_{22}^2+\phi_{22}\phi_{11})+\alpha\beta\mu S^*,\\
&\frac{\Delta_3^2\phi_{11}+\Delta_3^2\phi_{22}+\Delta_3\phi_{33}\phi_{44}+(\gamma+2\phi_{11}+\phi_{44})\alpha\beta S^*}{\Delta_3(\phi_{11}^2+\phi_{22}^2+\phi_{22}\phi_{11})+\alpha\beta\mu S^*}>1\\
&R_0>1
\end{aligned}$$

and hence, the EEP is stable if $R_0 > 1$. ■

3 Numerical Solution

By setting the variables

$$S=x_1, E=x_2, I_a=x_3, I_s=x_4, R=x_5, D=x_6$$

Then system of equations can be written as

$$\frac{dx_1}{dt} = \Lambda - \alpha\left(x_3 + x_4\right)x_1 - \mu x_1, \tag{3.1}$$

$$\frac{dx_2}{dt} = \alpha\left(x_3 + x_4\right)x_1 - \left(\beta + \mu + \delta\right)x_2, \tag{3.2}$$

$$\frac{dx_3}{dt} = p\beta x_2 + \gamma x_4 - \left(\lambda_1 + \mu + \eta\right)x_3, \tag{3.3}$$

$$\frac{dx_4}{dt} = \left(1-p\right)\beta x_2 - \left(\gamma + \lambda_2 + \eta + \mu\right)x_4, \tag{3.4}$$

$$\frac{dx_5}{dt} = \delta x_2 + \lambda_1 x_3 + \lambda_2 x_4 - \mu x_5, \tag{3.5}$$

$$\frac{dx_6}{dt} = \mu\left(x_1 + x_2 + x_3 + x_4 + x_5\right). \tag{3.6}$$

In order to simulate, it is assumed that there is no initial disease-related death or recovery and the other initial conditions are chosen based on the work of [21] as follows;

$$S\left(0\right) = 100; E\left(0\right) = 50; I_s\left(0\right) = 20; I_a\left(0\right) = 10; R\left(0\right) = 0; D\left(0\right) = 0.$$

The Runge-Kutta method is used to solve the system of differential equations (see [22, 23, 24, 25])

The parameter values are chosen as shown in Tables 1 and 2;

Table 1. Parameter choices

parameter	λ_1	λ_2	p	γ
values	0.36	0.36	Estimated	Estimated
Source	[26]		-	-

Table 2. Parameter choices

parameter	δ	α	β	η	μ
values	0.16	0.67	0.5	0.306	1/65
Source	[21]				

4 Analysis of Results and Discussion

The effects of intervention on the spread and containment of COVID-19 are analysed and discussed in this section.

Intervention in form awareness and public sensitisation is considered in this section. Increasing awareness and public sensitisation gives reduces the vulnerability of the susceptible class and thereby reduces the rate of interaction between infected and non-infected individual. Increasing intervention in terms awareness and public sensitisation means a reduction in the value of α. Fig. 4, shows that the Exposed Class increases with increasing α, and the Exposed class reduces as α decreases. A decrease in the Exposed class is experienced as α decreases because a proportion of the Susceptible Class recognises that interaction with an infected individual is a major means of transmission due to the awareness and public sensitisation. Also, as a consequence of the reduction in migration from Susceptible to the Exposed Class, the infected classes also reduce. This claim is verified by Figs. 5 and 6 where both the Symptomatic and Asymptomatic Infected classes reduce with time. In the long run, underlying COVID-19 death reduce significantly as shown in Fig. 7.

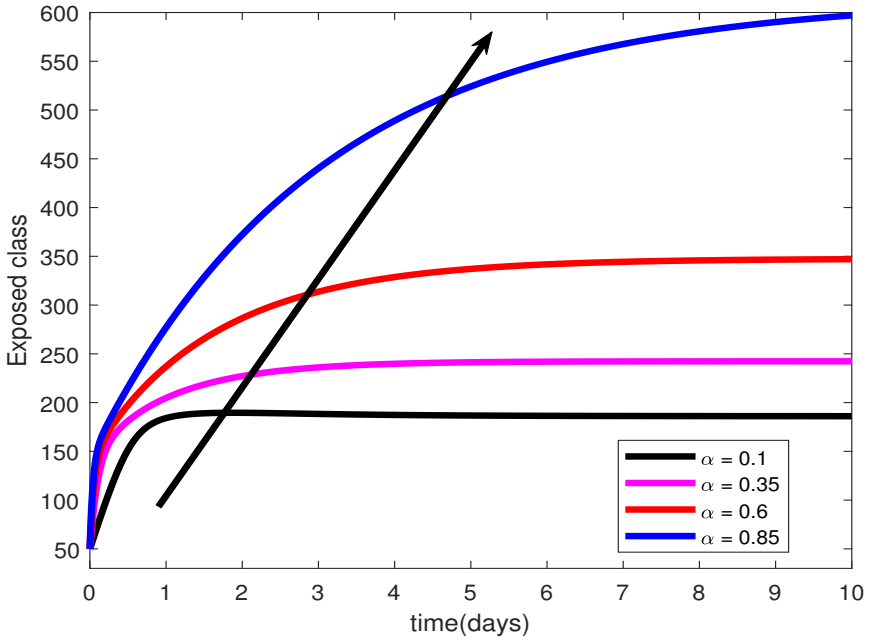

Fig. 4. Exposed class with α

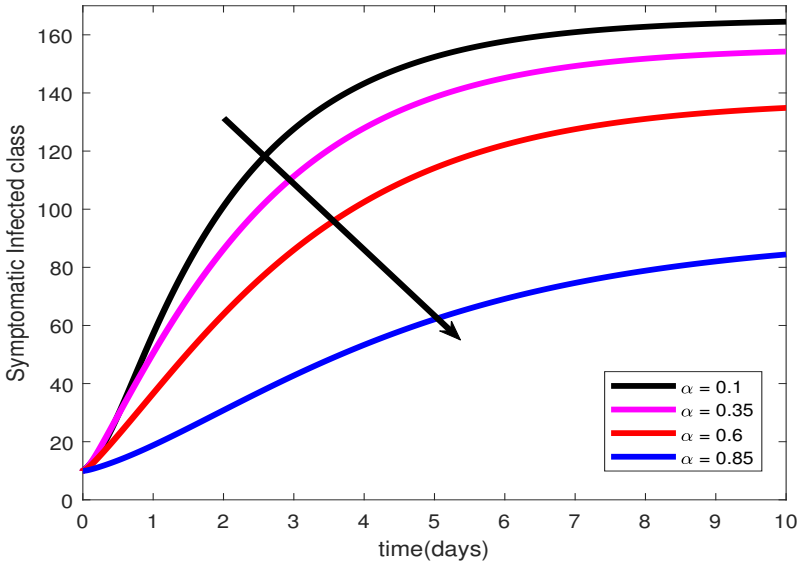

Fig. 5. Symptomatic Infected Class with α

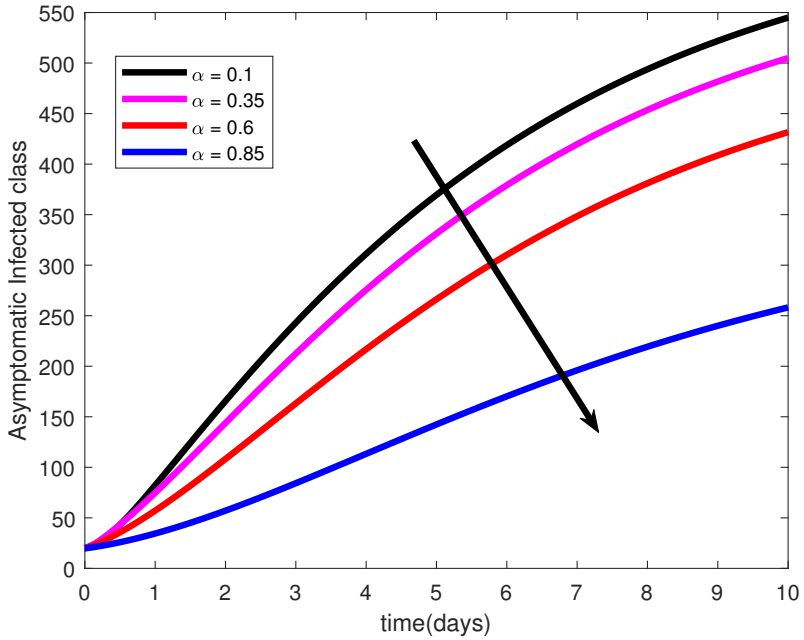

Fig. 6. Asymptomatic Infected Class with α

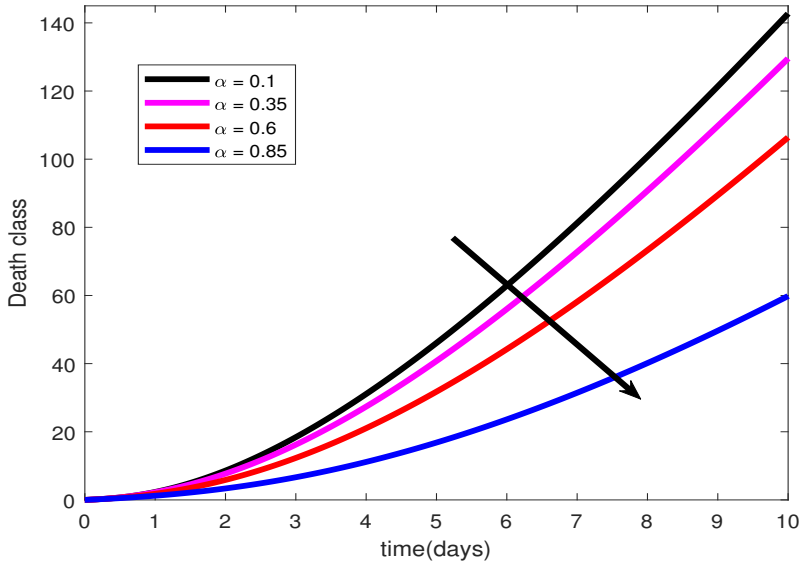

Fig. 7. Disease-Related Death Class with α

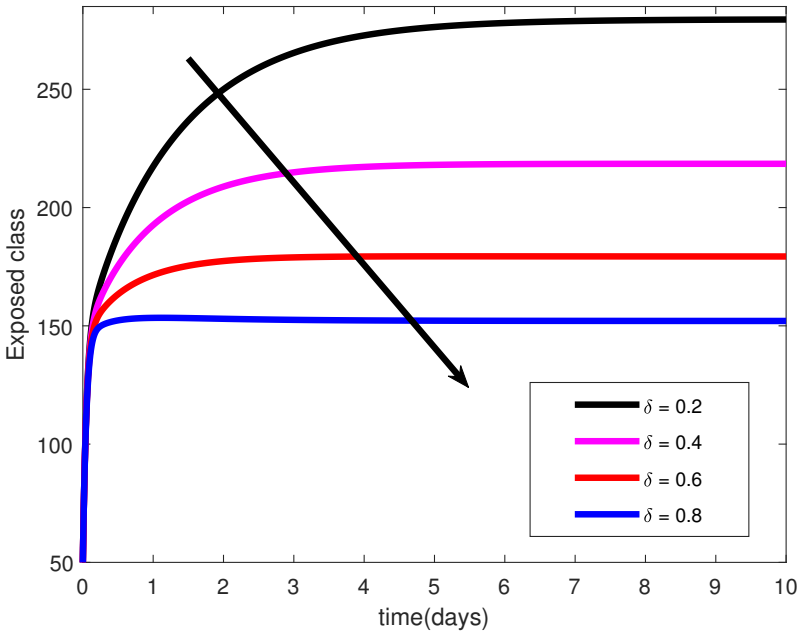

Fig. 8. Exposed with δ

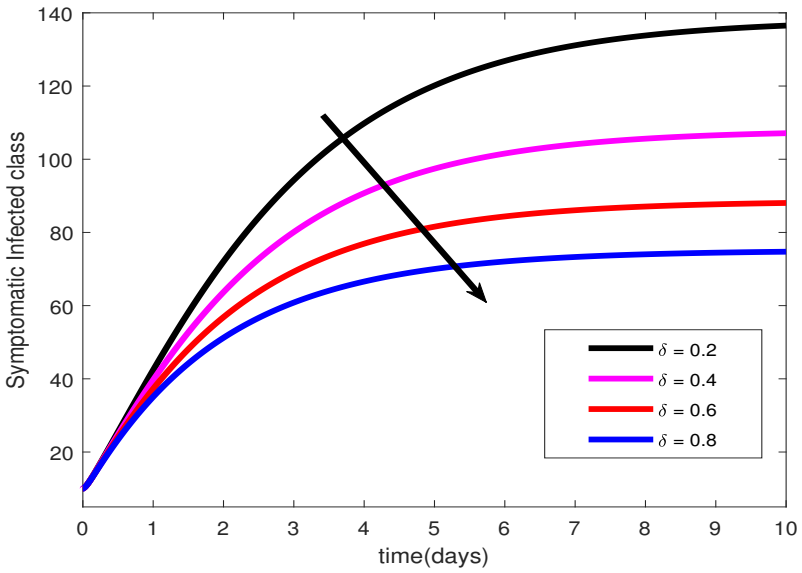

Fig. 9. Symptomatically Infected with δ

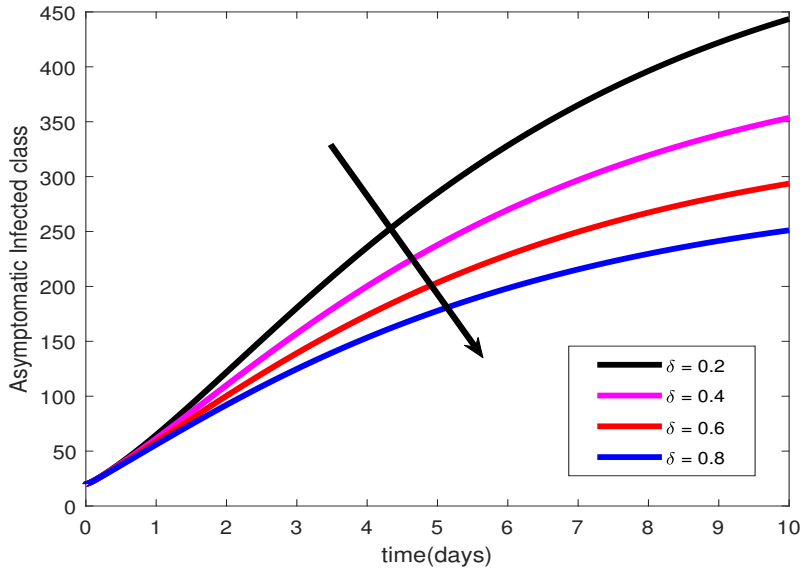

Fig. 10. Asymptomatically Infected Class with δ

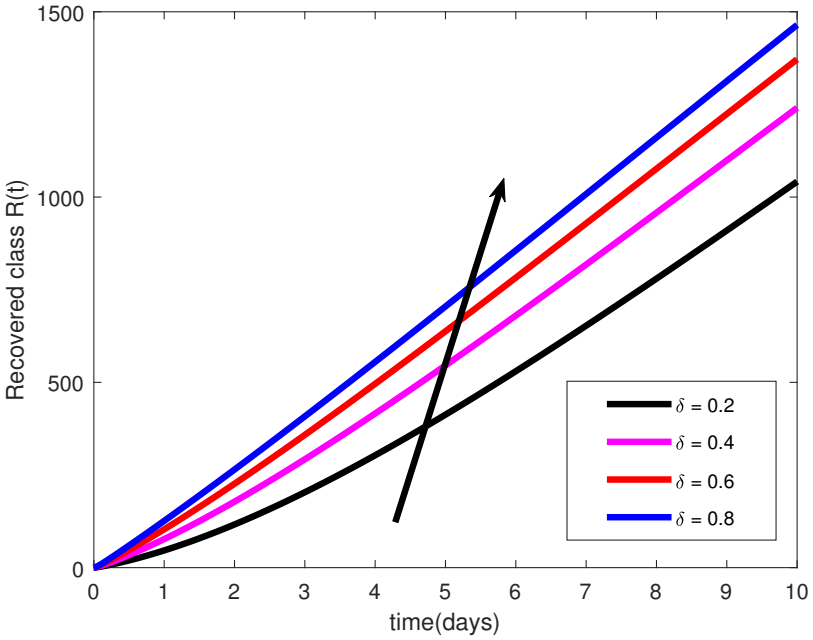

Fig. 11. Recovered Class with δ

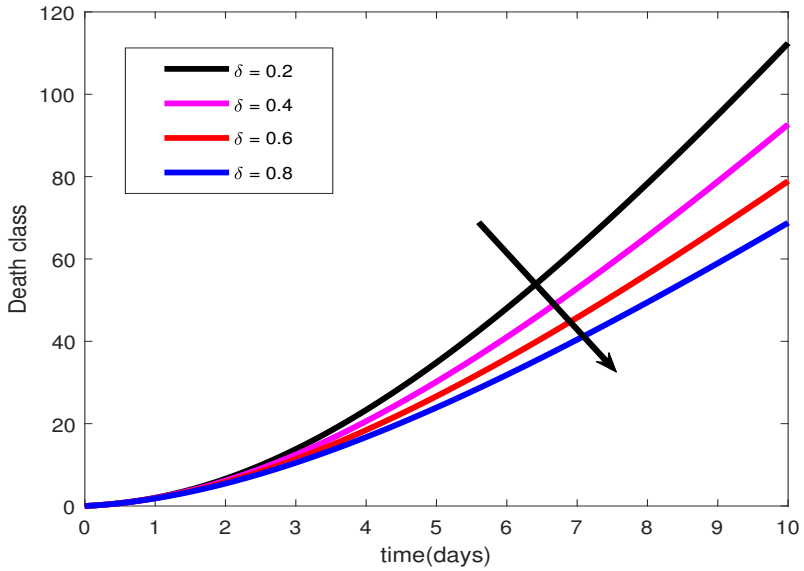

Fig. 12. COVID-19-Induced Death with δ

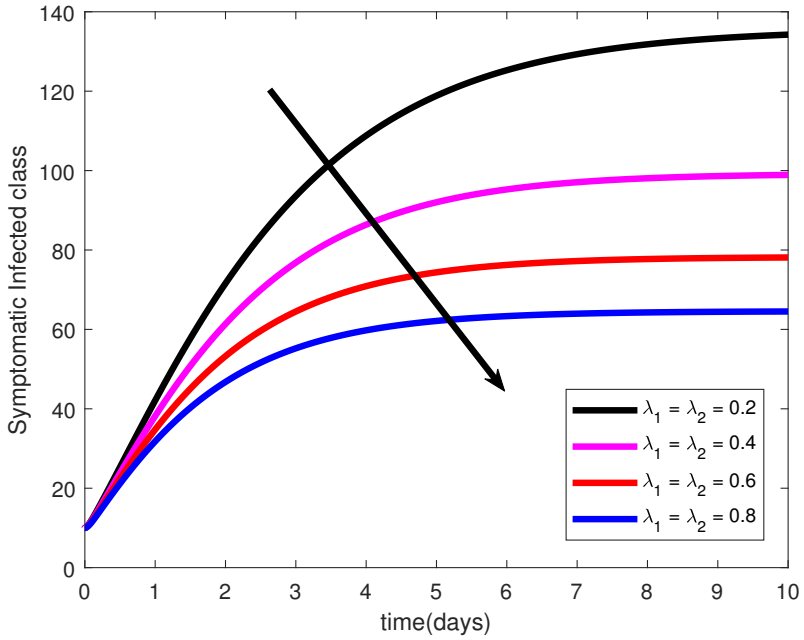

Fig. 13. Symptomatic Infected Class with λ

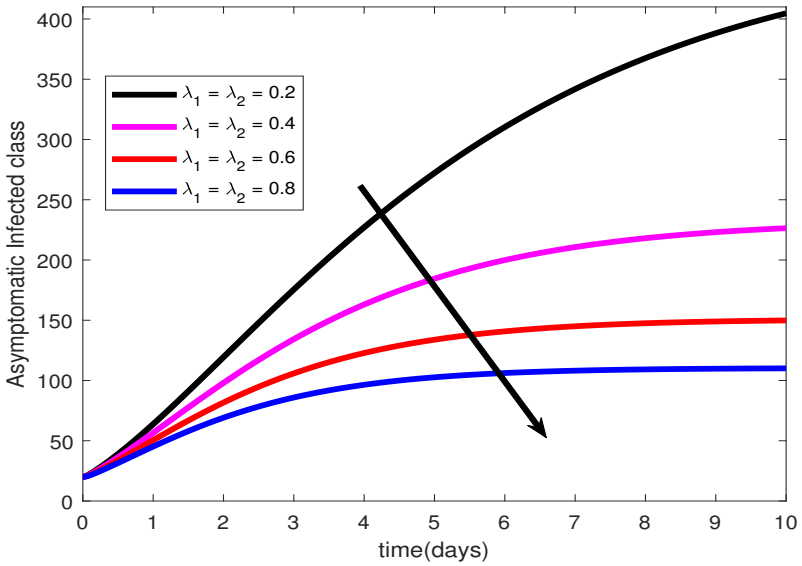

Fig. 14. Asymptomatic Infected Class with λ

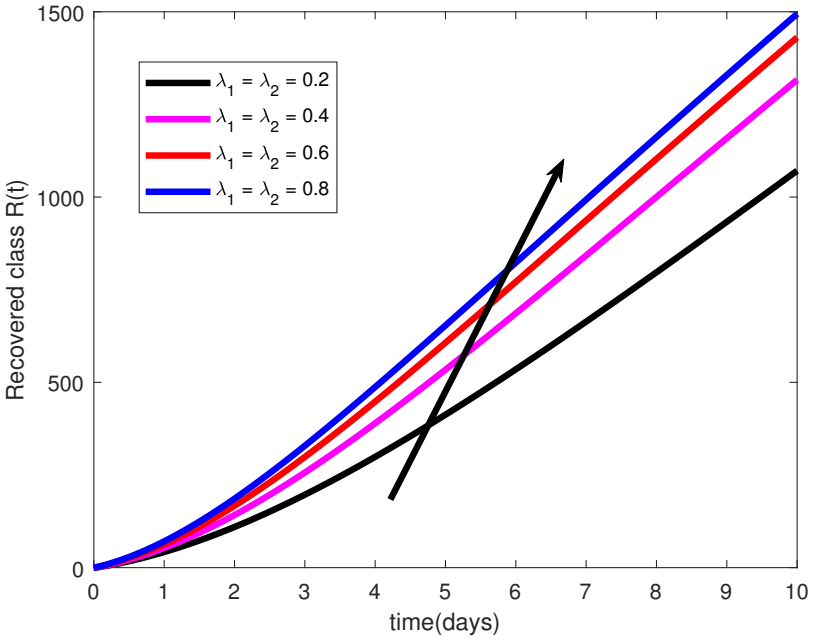

Fig. 15. Recovered Class with λ

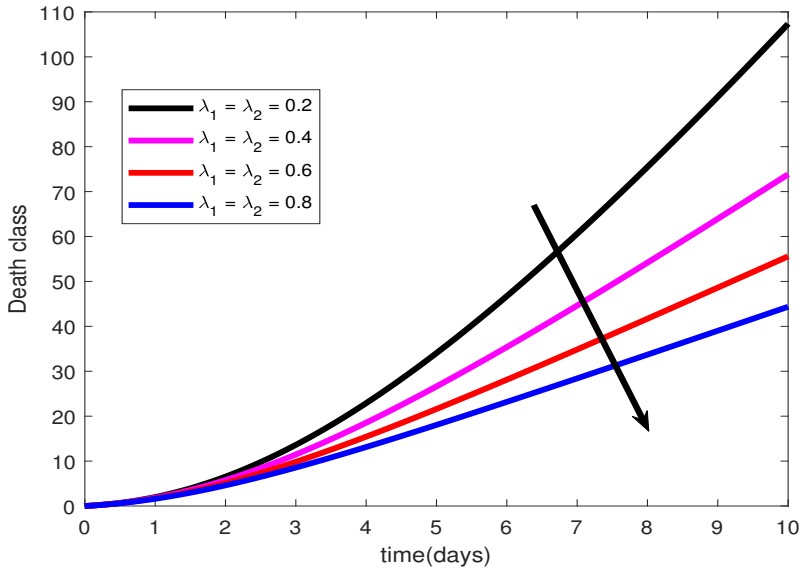

Fig. 16. COVID-19-Induced Death Class with λ

A susceptible individual who caught COVID-19 disease direct or indirectly will go through a window period when the disease through incubation. During this period, the individual does not test positive and is unable to transmit COVID-19 to any susceptible individual. Every individual in this category is classified into the Exposed Class. Increasing intervention in the form contact tracing and mass vaccination increases the rate of migration from the Exposed Class to the Recovered Class (i.e., increase in δ). Figs. 8-12, show the impact of increasing δ on COVID-19 dynamics in Kenya. Interventions in form of contact tracing provides rapid response to identify individuals who have exposed to COVID-19 but is not yet infected. Such individuals can be placed under surveillance and given proper monitoring. This will help to reduce the Exposed Class (this is supported by Fig 8. Figs 9 and 10, show that the infected classes reduce with increasing δ. This is due to the fact that Exposed individuals are identified before the disease becomes full-blown. Inclusion of mass vaccination will help move the some Exposed individuals directly to the Recovered class. This explains why Fig. 11 illustrates an increase in the individuals who get into the Recovered class. Clearly, once the recovered class increases, the COVID-19-induced death will also reduced Fig. 12.

Intervention in form of treatment to both Asymptomatic and Symptomatic Infected Classes has an increasing effects on the parameters λ_1 and λ_2. With treatment made available to all infected individuals, more individuals will migrate from the infected classes to the Recovered class. This will lead to a reduction in the infected classes Fig. 13 and 14, increase in the recovered class Fig. 15 and a decrease in the COVID-19-induced deaths Fig. 16.

5 Conclusion

This study analyses the effects of intervention on COVID-19 dynamics. Equations governing the spread of COVID-19 are formulated by using the SEIRD model, where the Infected class is further classified as Asymptomatic and Symptomatic classes. The disease-free and endemic equilibrium points of the model are obtained and their stability conditions are established. The reproduction number R_0 for the model is also obtained and the equilibrium points are found to be stable if $R_0 < 1$. The model is analysed and the results are depicted as graphs.

The result from this study show that:

1. Intervention in form awareness and public sensitisation reduces the Exposed class, Infected Classes and COVID-19-related death.
2. Intervention in the form contact tracing and mass vaccination reduces the Exposed class, Infected Classes and COVID-19-related death but increases Recovery Class.
3. Intervention in form of treatment to Infected classes reduces the Infected Classes and COVID-19-induced deaths while increasing the recovered class.

Interventions in form of contact tracing and mass vaccination for early detection of infections and availability of immediate treatment for any detected case will help reduce the spread of COVID-19 in Kenya.

Competing Interests

Authors have declared that no competing interests exist.

References

[1] Monto AS. Coronaviruses. The Yale Journal of Biology and Medicine. 1974;47:234-251.

[2] Lai MM, Holmes KV. Coronaviridae: the viruses and their replication. In eds. F. Virology (Ed.). In: Knipe DM, Howley PM Philadelphia, PA: Lippincott-Raven. Published online 2001.

[3] Who. Coronavirus disease 2019 (COVID-19) Situation Report - 40. World Health Organisation; 2020.

[4] Faïçal Ndaïrou, Torres DFM. Mathematical Analysis of a Fractional COVID-19 Model Applied to Wuhan, Spain and Portugal. Axioms. 2021;10(3):135.

[5] Tyrrell DAJ, Bynoe ML. Cultivation of viruses from a high proportion of patients with colds. The Lancet. 1966;287(7428):76-77.

[6] Hamre D, Procknow JJ. A New Virus Isolated from the Human Respiratory Tract. Experimental Biology and Medicine. 1966;121(1):190-193.

[7] McIntosh K, Becker WB, Chanock RM. Growth in suckling-mouse brain of 'IBV-like' viruses from patients with upper respiratory tract disease. Proceedings of the National Academy of Sciences. 1967;58(6):2268-2273.

[8] Kahn JS, McIntosh K. History and Recent Advances in Coronavirus Discovery. Pediatric Infectious Disease Journal. 2005;24(11):S223-S227.

[9] Oke AS, Bada OI, Rasaq G, Adodo V. Mathematical analysis of the dynamics of COVID-19 in Africa under the influence of asymptomatic cases and re-infection. Mathematical Methods in the Applied Sciences. 2021;45(1):137-149.

[10] Dos Santos WG. Natural history of COVID-19 and current knowledge on treatment therapeutic options. Biomedicine Pharmacotherapy. 2020;129:110493.

[11] Shahrear P, Rahman SMS, Nahid MMH. Prediction and mathematical analysis of the outbreak of coronavirus (COVID-19) in Bangladesh. Results in Applied Mathematics. 2021;10:100145.

[12] Tchoumi SY, Rwezaura H, Diagne ML, González-Parra G, Tchuenche J. Impact of Infective Immigrants on COVID-19 Dynamics. Mathematical and Computational Applications. 2022;27(1):11.

[13] Andima RN, Mutuku WN, Farai N, Awuor K, Oke AS. Impact of Fixed Allocation of Health Resources on Diabetes in Kenya: Mathematical Modelling Approach. Advances in Applied Sciences. 2022;7(4):125-134.

[14] Andima RN, Mutuku WN, Farai N, Awuor K, Oke AS. Mathematical Modelling of Diabetes under a Constrained Hospitalisation Resources. OALib. 2022;09(10):1-14.

[15] Bada OI, Oke AS, Mutuku WN, Aye PO. Analysis of the Dynamics of SI-SI-SEIR Avian Influenza A(H7N9) Epidemic Model with Re-infection. Earthline Journal of Mathematical Sciences. Published online July 2020:43-73.

[16] Kimulu AM, Mutuku WN, Mwalili SM, Malonza D, Oke AS. Mathematical Modelling of the Effects Funding on HIV Dynamics Among Truckers and Female Sex Workers Along the Kenyan Northern Corridor Highway. Advances in Applied Sciences. 2022;7(3):52-64.

[17] Kimulu AM, Mutuku WN, Mwalili SM, Malonza D, Oke AS. Male Circumcision: A Means to Reduce HIV Transmission between Truckers and Female Sex Workers in Kenya. Journal of Mathematical Analysis and Modeling. 2022;3(1):50-59.

[18] Ates M. Circuit theory approach to stability and passivity analysis of nonlinear dynamical systems. International Journal of Circuit Theory and Applications. 2021;50(1):214-225. doi:10.1002/cta.3159

[19] Oke AS, Bada OI. Analysis of the dynamics of avian influenza A(H7N9) epidemic model with re-infection. Open Journal of Mathematical Sciences. 2019;3(1):417-432.

[20] Zafar ZUA, Hussain MT, Inc M, et al. Fractional-order dynamics of human papillomavirus. Results in Physics. 2022;34:105281.

[21] Mbogo RW, Orwa TO. SARS-COV-2 outbreak and control in Kenya - Mathematical model analysis. Infectious Disease Modelling. 2021;6:370-380.

[22] Oke A. Convergence of Differential Transform Method for Ordinary Differential Equations. Journal of Advances in Mathematics and Computer Science. 2017;24(6):1-17.

[23] Oke AS, Fatunmbi EO, Animasaun IL, Juma BA. Exploration of ternary-hybrid nanofluid experiencing Coriolis and Lorentz forces: case of three-dimensional flow of water conveying carbon nanotubes, graphene, and alumina nanoparticles. Waves in Random and Complex Media. Published online September 2022:1-20.

[24] Okundalaye OO, Othman WAM, Oke AS. Toward an efficient approximate analytical solution for 4-compartment COVID-19 fractional mathematical model. Journal of Computational and Applied Mathematics. 2022;416:114506.

[25] Juma BA, Oke AS, Mutuku WN, Ariwayo AG, Ouru OJ. Dynamics of Williamson fluid over an inclined surface subject to Coriolis and Lorentz forces. Engineering and Applied Science Letter. 2022;5(1):37-46.

[26] Mumbu AJ, Hugo AK. Mathematical modelling on COVID-19 transmission impacts with preventive measures: a case study of Tanzania. Journal of Biological Dynamics. 2020;14(1):748-766.

Peer-review history:
The peer review history for this paper can be accessed here (Please copy paste the total link in your browser address bar)
https://www.sdiarticle5.com/review-history/94692